NASA Technical Paper 1053

Friction and Deformation Behavior of Single-Crystal Silicon Carbide

Kazuhisa Miyoshi and Donald H. Buckley

OCTOBER 1977

NASA

NASA Technical Paper 1053

Friction and Deformation Behavior of Single-Crystal Silicon Carbide

Kazuhisa Miyoshi
Kanazawa University
Kanazawa, Japan
and
Donald H. Buckley
Lewis Research Center
Cleveland, Ohio

National Aeronautics
and Space Administration

**Scientific and Technical
Information Office**

1977

FRICTION AND DEFORMATION BEHAVIOR OF SINGLE-CRYSTAL SILICON CARBIDE

by Kazuhisa Miyoshi* and Donald H. Buckley

Lewis Research Center

SUMMARY

The friction and deformation behavior of single-crystal silicon carbide was investigated to determine the effects of the orientation of the silicon carbide on friction and deformation. Sliding friction experiments were conducted with a diamond rider sliding on a single-crystal silicon carbide (0001) surface in the $\langle 10\bar{1}0 \rangle$ and $\langle 11\bar{2}0 \rangle$ directions. Both spherical and conical diamond riders were used. All experiments were conducted with light loads of 5 to 50 grams at a sliding velocity of 3 mm/min in argon at atmospheric pressure.

When the radius of curvature of the spherical diamond rider was large (0.3 mm), deformation of silicon carbide was primarily elastic. Under these conditions the friction coefficient was low and did not show a dependence on the orientation of the silicon carbide. Further, there was no detectable cracking of the silicon carbide surfaces. When smaller radii of curvature of the spherical diamond rider (0.15 and 0.02 mm) or a conical diamond rider was used, plastic grooving occurred, the silicon carbide exhibited anisotropic friction and deformation behavior, and the friction coefficient depended on load. Anisotropic friction and deformation of the basal plane of silicon carbide was controlled by the slip system $\{10\bar{1}0\}\langle 11\bar{2}0 \rangle$ and cleavage of $\{10\bar{1}0\}$. It is predicted from the foregoing conclusions that the $\langle 10\bar{1}0 \rangle$ direction in the basal plane of silicon carbide will exhibit the greatest resistance to abrasion in practical applications.

---

*Assistant Professor of Precision Engineering, Kanazawa University, Kanazawa, Japan; National Research Council - National Aeronautics and Space Administration Research Associate.

INTRODUCTION

It has been anticipated that silicon carbide, because of its very high hardness (9 on Moh's scale), will be highly resistant to abrasion in an unlubricated environment (ref. 1). However, detailed examination of single-crystal silicon carbide in sliding contact with titanium revealed evidence of silicon carbide wear debris. Further wear debris plows the silicon carbide surface itself, and grooves are produced in a plastic manner on the surface (ref. 2). Thus, it would be of interest to know the friction deformation and fracture behavior of silicon carbide, which is inherently brittle when compared with metals. In addition, knowledge of the influence of crystallographic orientation on the friction and deformation behavior of silicon carbide may lead to a better abrasion-resistant material for practical applications. Wear of abrasives such as silicon carbide occurs in such operations as grinding, and it is highly desirable to minimize this wear.

This investigation was conducted to examine the friction and deformation behavior of single-crystal silicon carbide in contact with a diamond rider. The orientation of silicon carbide was also examined relative to its effect on friction and deformation. All experiments were conducted with light loads of 5 to 50 grams at a sliding velocity of 3 mm/min in dry argon ($H_2O < 20$ ppm) at atmospheric pressure on the (0001) basal plane in the $\langle 10\bar{1}0 \rangle$ and $\langle 11\bar{2}0 \rangle$ directions. Both spherical and conical diamond riders were used. The silicon carbide was subjected to single-pass sliding by a diamond rider; the sliding distance was 2 mm. Studies were all at room temperature.

MATERIALS

The single-crystal silicon carbide platelets used in these experiments were a 99.9-percent-pure compound of silicon and carbon. Silicon carbide (ref. 3) has a hexagonal close-packed crystal structure with unit cell dimensions in the most commonly occurring form of $a = 3.0817$ Å and $c = 15.1183$ Å. The c direction was perpendicular to the sliding interface with the basal plane and therefore parallel to the interface. The Knoop hardness was 2954 in the $\langle 10\bar{1}0 \rangle$ direction and 2917 in the $\langle 11\bar{2}0 \rangle$ direction on the basal plane of silicon carbide (ref. 4).

The diamonds were commercially purchased. With the possible exception of the artifically formed cubic modification of boron nitride, diamond is the hardest known material (ref. 5). It indents silicon carbide without itself suffering permanent deformation. Also, its elastic constants are very high. Young's modulus for silicon carbide is about 4.5×10^5 N/mm^2 (ref. 6), for diamond it lies between 7×10^5 and 10×10^5 N/mm^2 (ref. 7). At low sliding velocity in argon at atmospheric pressure, the adhesion of diamond to silicon carbide is very low.

APPARATUS

The apparatus used in this investigation was a system capable of applying load and measuring friction in argon at atmospheric pressure. The mechanism for measuring friction is shown schematically in figure 1. The beam contains one flat machined normal to the direction of friction application. The end of the rod contains the diamond rider. The load is applied by placing deadweights on a pan on top of the rod. Under an applied load the friction force is sensed by strain gages.

EXPERIMENTAL PROCEDURE

The single-crystal silicon carbide surfaces were mechanically polished with 1-μm aluminum oxide (Al_2O_3) powder (ref. 2). The diamond riders were both spherical and conical. Three radii of curvature of the spherical riders were used: 0.02, 0.15, and 0.3 mm. The apical angle of the conical riders was about 120°, and the radius of curvature at the apex was less than 5 μm. These riders were polished with Al_2O_3 before each friction experiment. Both the silicon carbide and diamond surfaces were rinsed with water and 200-proof ethyl alcohol prior to use. The friction experiments were single pass. Experiments were conducted with a total sliding distance of 2 mm at a sliding velocity of 3 mm/min.

RESULTS AND DISCUSSION

Friction and Elastic Deformation with a Spherical Diamond Rider

Sliding friction experiments were conducted with a 3-mm-radius spherical diamond rider in contact with a flat silicon carbide (0001) surface. The friction coefficients measured at various loads are presented in figure 2. The data of figure 2 indicate that the friction coefficient was not constant but decreased as the load increased. Friction was generally very low and does not seem to be dependent on silicon carbide orientation. The friction coefficient was about 0.08 at a load of 5 grams and decreased to about 0.03 at a load of 50 grams. Thus, it might be concluded that the sliding truly occurred at the interface and that an elastic deformation could occur in both the silicon carbide and the diamond, which would account for the low friction observed. To a first approximation for this load range, the relation between friction coefficient μ and load W is given by an expression of the form $\mu = KW^{c-1}$ ($c - 1 \approx -1/3$). The minus 1/3 power can be interpreted most simply as arising from an adhesion mechanism, the area of contact being determined by elastic deformation as was observed herein and in reference 5. Even at

high magnifications (up to 10 000) of the scanning electron microscope, no groove formation due to plastic flow and no cracking of silicon carbide with sliding was observed. The friction results obtained herein with a 0.3-mm-radius spherical diamond rider in sliding contact with silicon carbide show that silicon carbide primarily deforms elastically. Over the entire load range, as a rough estimate, the mean contact pressure was 150 to 350 kg/mm^2. The maximum pressure at the center according to Hertz (ref. 8) would thus be 230 to 490 kg/mm^2 (table I).

Friction and Plastic Deformation with Spherical Diamond Rider

Sliding friction experiments were conducted with 0.15- and 0.02-mm-radius spherical diamond riders in contact with a flat silicon carbide surface (on the (0001) plane in the $\langle 11\bar{2}0 \rangle$ direction). The friction coefficients measured at various loads are presented in figure 3. The friction was not constant but increased as the load increased. To a first approximation for this load range, the relation between friction coefficient μ and load W is given by the expression $\mu = KW^{c-1}$. The index c depends on the rider radius of curvature. The value of c is approximately 1.3 for rider radii of 0.02 and 0.15 mm.

The friction coefficients measured with the various rider radii of curvature (0.02, 0.15, and 0.3 mm) showed that the friction behavior differed markedly with radius of curvature. In these experiments, when c is less than 1.0, deformation is primarily elastic; when c is greater than 1.0, deformation is plastic.

With diamond riders of 0.15- and 0.02-mm radii in sliding contact with flat silicon carbide surfaces and c greater than 1.0, it might be anticipated that plastic deformation would occur in the silicon carbide (ref. 9). The spherical diamond rider would then plow out silicon carbide from the flat. The calculated mean contact pressure at a 50-gram load with a 0.02-mm-radius rider would be about 2000 kg/mm^2. The maximum pressure at the center would be about 3000 kg/mm^2 (i.e., the yield pressure of silicon carbide (table I)).

The experimental evidence establishes that permanent grooves in silicon carbide are formed during sliding, as evident in figure 4. Figure 4 presents surface replication electron micrographs of a wear track generated by a 0.02-mm-radius spherical diamond rider at loads of 30 and 40 grams. It becomes obvious from an examination of figure 4 that a degree of plastic deformation occurred in the silicon carbide. Surface cracking was observed at loads of 30 and 40 grams. At a 40-gram load, however, two types of cracking were observed. One type is characterized by a very small crack (P in fig. 4(b)) in the wear track that propagated perpendicular to the sliding direction. The other is a crack (S in fig. 4(b)) on both sides of the wear track that propagated outward

from the wear track. Some cracks zigzagged along cleavage planes of $\{10\bar{1}0\}$ in the $\langle 11\bar{2}0\rangle$ directions (Z in fig. 4(b)).

With a 0.02-mm-radius rider and a load of less than 20 grams, no cracks were observed. With a load of more than 30 grams, however, cracks were visible, as shown in figure 4. The first sign of cracking was the formation of a crack in the wear track (top of fig. 4(a)). Thus, the critical load for crack formation during sliding was 30 grams.

When a 0.15-mm-radius rider was used in these same experiments, small permanent grooves were formed in the silicon carbide during sliding. However, no cracks were visible. These observations and the friction results with a 0.15-mm-radius diamond rider in sliding contact with silicon carbide show that silicon carbide can deform both elastically and plastically and that the spherical diamond rider then plows the silicon carbide surface.

The measured friction coefficients were also orientation dependent (see section Anisotropies of Friction and Deformation on Basal Plane and fig. 10). This dependence reveals that the friction coefficient is influenced by the bulk properties of silicon carbide. The subject is explained in detail in the next section.

Friction, Plastic Deformation, and Cracking with Conical Diamond Rider

Sliding friction experiments were conducted with conical diamond riders in contact with a flat silicon carbide (0001) surface. Friction traces measured at various loads are presented in figure 5. The friction traces for light loads of 5, 10, and 20 grams are characterized by randomly fluctuating behavior, with no evidence or only occasional evidence of stick-slip behavior. On the other hand, the traces for heavy loads of 30, 40, and 50 grams are primarily characterized by a continuous, marked stick-slip behavior.

The friction coefficient was generally low (<0.4) when stick-slip was absent (see average fluctuating friction in fig. 6). In this case, the sliding appears to involve a plastic flow and a small amount of cracking, as shown in figure 7. Figure 7 contains a scanning and a surface replication electron micrograph of wear tracks that were generated by a conical diamond rider at a load of 30 grams. It becomes obvious from an examination of figure 7 that a significant degree of plastic deformation occurred in the silicon carbide. It has been suggested that the plastic behavior of otherwise brittle materials is due to the high compressive stress that exists at the front contact surface of the rider during sliding (refs. 5 and 9). Under such conditions, sliding occurs at the interface and the friction primarily involves shearing at the interface and plowing (plastic deformation) in silicon carbide.

By contrast, the friction coefficient, which shows a marked stick-slip behavior, was high (see average maximum peak height in fig. 6). This friction process was accompanied by both gross surface cracking and plastic flow, as shown in figure 8. Figure 8

presents scanning electron micrographs of the wear track generated by a conical diamond rider sliding at a 50-gram load. Considerable fracture of the surface occurred as a result of cleavage. In addition, the heavily deformed groove in the central portion of the wear track was caused by plastic flow. The fracturing of the silicon carbide surface (fig. 8) is the result of cracks being generated along $\{10\bar{1}0\}$ and $\{0001\}$ planes, propagating, and then intersecting. Thus, surface cracking in figure 8 is primarily due to cleavage of $\{10\bar{1}0\}$ planes, with the subsurface cracking being caused by cleavage along $\{0001\}$ planes. Under such conditions, large amounts of wear debris are generated during sliding (fig. 9). Figure 9 presents optical micrographs of wear tracks showing fragments of silicon carbide. Figure 9 also reveals light areas adjacent to the wear track that are due to slip-step or subsurface cracking generated during sliding.

Increasing the load resulted in increased fracture. With heavier loads, the friction coefficient increased to its equilibrium value of 0.6 to 0.9. This value depends on the sliding direction, as indicated in figure 6.

The foregoing results reveal that plastic flow, cleavage, and fracture in silicon carbide are the main factors responsible for the observed friction behavior. Further, these studies show that the friction coefficient is influenced by the bulk properties of silicon carbide (friction dependency on orientation).

Anisotropies of Friction and Deformation on Basal Plane

The friction coefficient was measured as a function of the crystallographic direction of sliding on the basal plane (0001) of silicon carbide for various diamond riders. The results obtained are presented in figure 10. Anisotropy is governed by two factors: the geometry of the rider and the load. When the radius of curvature of the spherical rider was made larger or a lighter load was applied to the sliding surface (i.e., elastic deformation or a small amount of plastic flow occurred), the friction was low. Further, the anisotropy diminished as indicated by the results of a 0.3-mm-radius spherical diamond rider sliding at loads of 5 and 30 grams and a 0.02-mm-radius rider sliding at a load of 5 grams (fig. 10). This type of behavior was also observed with diamond in sliding contact with itself (ref. 3).

When higher loads were applied to the 0.02-mm-radius spherical rider or a conical rider was used, penetration of the bulk occurred as a result of gross plastic flow and the silicon carbide exhibited anisotropic friction and deformation behavior. Observations of the silicon carbide surface by optical, scanning electron, and replication electron microscopy indicated that the $\langle 11\bar{2}0\rangle$ direction had the larger wear track because of plastic flow and was the direction of high friction. This is the soft direction on the silicon carbide (0001) single-crystal surface.

Microhardness studies by Shaffer (ref. 4) and Adewoye, et al., (ref. 3) also show a similar small anisotropy, with greater Knoop hardness in the $\langle 10\bar{1}0 \rangle$ direction than in the $\langle 11\bar{2}0 \rangle$ direction. The Knoop hardness of the basal plane of silicon carbide was greater than that for any other crystallographic plane in the material (ref. 4). It was therefore, anticipated that the $\langle 10\bar{1}0 \rangle$ direction in the basal plane of silicon carbide would exhibit the greatest abrasion resistance in practical applications because bulk deformation plays a role in the frictional anisotropy of silicon carbide.

Silicon carbide specimen surfaces on which a conical diamond rider slid in the $\langle 1010 \rangle$ direction were etched with molten salt ($1NaF + 2KCO_3$) at 700° to 800° C to reveal dislocations. These surfaces are shown in figure 11. Observations of the surface confirm that plastic flow has taken place beyond the actual wear track. In several cases, straight rows of dislocation etch pits appear along the $\langle 11\bar{2}0 \rangle$ direction in the (0001) plane. This is confirmatory evidence that the $\{10\bar{1}0\} \langle 11\bar{2}0 \rangle$ slip system is operating during sliding. This slip system is then responsible for the frictional anisotropy observed on the basal plane of silicon carbide.

Several slip systems have been observed in ∂-silicon carbide, such as (0001) $\langle 11\bar{2}0 \rangle$, $\{3\bar{3}01\} \langle 11\bar{2}0 \rangle$ (ref. 10), and $\{10\bar{1}0\} \langle 11\bar{2}0 \rangle$ (ref. 11). The deformation behavior of silicon carbide during sliding, as mentioned previously, may be readily explained in terms of the resolved shear stresses (ref. 12) acting on $\{10\bar{1}0\} \langle 11\bar{2}0 \rangle$ slip systems during slidings in the $\langle 10\bar{1}0 \rangle$ and $\langle 11\bar{2}0 \rangle$ directions on a (0001) silicon carbide surface. In addition, Adewoye, et al., (ref. 3) explained the Knoop hardness anisotropy data for the (0001) plane of ∂-SiC by using the resolved shear stress analysis (ref. 12). Similar data for Knoop hardness anisotropy of tungsten carbide have been explained by a resolved shear stress calculation involving the $\{10\bar{1}0\} \langle 0001 \rangle$ and $\{10\bar{1}0\} \langle 11\bar{2}0 \rangle$ slip systems (ref. 12).

CONCLUSIONS

From the sliding friction experiments conducted in this investigation with single-crystal silicon carbide in sliding contact with spherical and conical diamond riders, the following conclusions were drawn:

1. When the radius of curvature of the spherical diamond rider is large (0.3 mm), deformation of silicon carbide is principally elastic. Under these conditions the friction coefficient is low and does not show a dependence on the orientation of the silicon carbide. Further, there is no detectable cracking of the silicon carbide surfaces.

2. Where the radius of curvature of the spherical diamond rider is smaller (0.15 and 0.02 mm) or a conical diamond rider is used, plastic grooving occurs, silicon carbide exhibits anisotropic friction and deformation behavior, and the friction coefficient depends on load.

3. Anisotropic friction and deformation on the basal plane of silicon carbide is controlled by the slip system $\{10\bar{1}0\}\langle 11\bar{2}0\rangle$ and a cleavage of $\{10\bar{1}0\}$.

It is predicted from the foregoing conclusions that the $\langle 10\bar{1}0\rangle$ directions in the basal plane of silicon carbide will exhibit the greatest resistance to abrasion in practical applications.

Lewis Research Center,
National Aeronautics and Space Administration,
Cleveland, Ohio, June 17, 1977,
506-16.

REFERENCES

1. Buckley, Donald H.: Friction, Wear and Lubrication in Vacuum. NASA SP-277, 1971.

2. Miyoshi, Kazuhisa; and Buckley, Donald H.: Friction and Wear Behavior of Single-Crystal Silicon Carbide in Contact with Titanium. NASA TN , 1977.

3. Adewoye, O. O.; et al.: Structural Studies of Surface Deformation in MgO, SiC and Si_3N_4. Univ. Cambridge, (AD-A008993), 1974.

4. Shaffer, Peter T. B.: Effect of Crystal Orientation on Hardness of Silicon Carbide. J. Amer. Ceram. Soc., vol. 47, no. 9, Sept. 1964, p. 466.

5. Bowden, F. P.; and Tabor, D.: The Friction and Lubrication of Solids. Part II. Clarendon Press (London), 1964.

6. Hasselman, D. P. H.; and Batha, H. D.: Strength of Single Crystal Silicon Carbide. Appl. Phys. Lett., vol. 2, no. 6, Mar. 15, 1963, pp. 111-113.

7. Bhagavantam, S.; and Bhimasenachar, J.: Elastic Constants of Diamond. Proc. R. Soc. London, Ser. A, vol. 187, no. 1010, Nov. 5, 1946, pp. 381-384.

8. Bowden, F. P.; and Tabor, D.: The Friction and Lubrication of Solids. Part I. Clarendon Press (London), 1950.

9. Tanaka, K.; et al.: Friction and Deformation of Mn-Zn Ferrite Single Crystals. Proceedings of the JSLE-ASLE International Lubrication Conference, Tokyo, 1975, T. Sakurai, ed., Elsevier Scientific Publishing Co., 1976, pp. 58-66.

10. Amelinckx, S.; Strumane, G.; and Webb, W. W.: Dislocations in Silicon Carbide. J. Appl. Phys., vol. 31, no. 8, Aug. 1960, pp. 1359-1370.

11. Brookes, C. A.; O'Neill, J. B.; and Redfern, B. A. W.: Anisotropy in the Hardness of Single Crystals. Proc. R. Soc., London, Ser. A, vol. 322, no. 1548, Mar. 23, 1971, pp. 73-88.

12. French, David N.; and Thomas, David A.: Hardness Anisotropy and Slip in WC Crystals. Trans. Metall. Soc. AIME, vol. 233, no. 5, May 1965, pp. 950-952.

TABLE I. - MAXIMUM HERTZIAN CONTACT STRESS OF SILICON CARBIDE IN STATIC CONTACT WITH DIAMOND RIDERS

Normal load, g	Radius of curvature of rider, mm		
	0.02	0.15	0.3
	Maximum Hertzian contact stress, kg/mm^2		
5	14×10^2	3.7×10^2	2.3×10^2
10	18	4.6	2.9
20	22	5.8	3.7
30	25	6.6	4.2
40	28	7.3	4.6
50	30	7.8	4.9

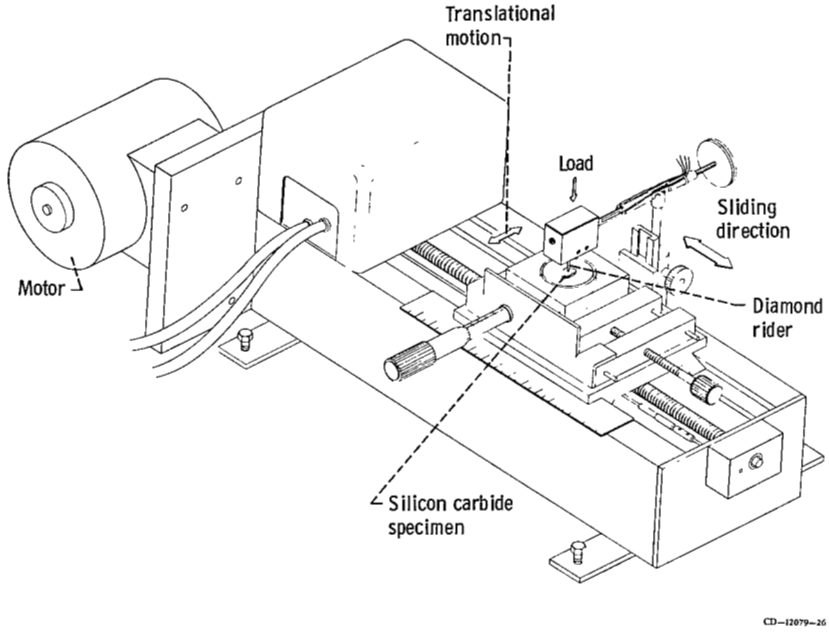

Figure 1. - Friction and wear apparatus in argon at atmospheric pressure.

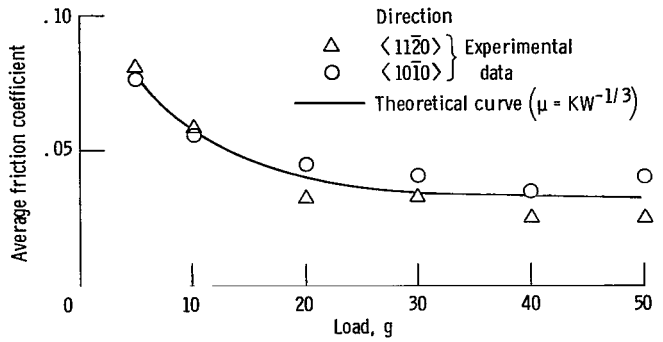

Figure 2. - Average friction coefficient as function of load for a spherical 0.3-mm-radius diamond rider sliding on silicon carbide (0001) single-crystal surface in argon at atmospheric pressure. Sliding velocity, 3 mm/min; temperature, 25° C.

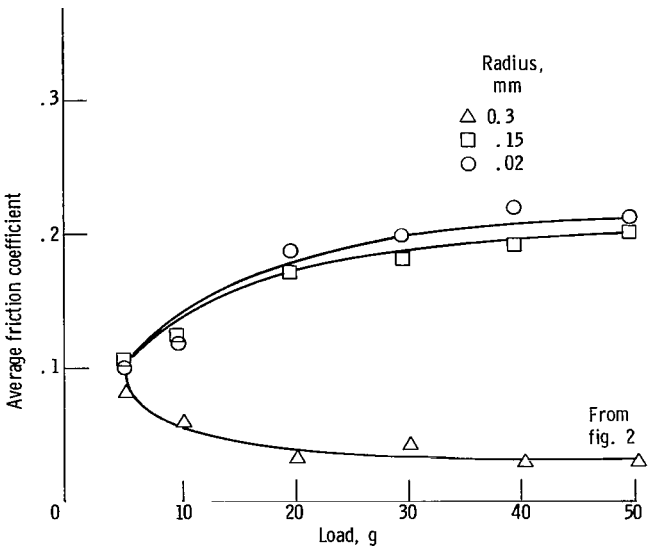

Figure 3. - Average friction coefficient as function of load for spherical diamond riders sliding on silicon carbide (0001) single-crystal surface in argon at atmospheric pressure. Sliding direction, ⟨11$\bar{2}$0⟩; sliding velocity, 3 mm/min; temperature, 25° C.

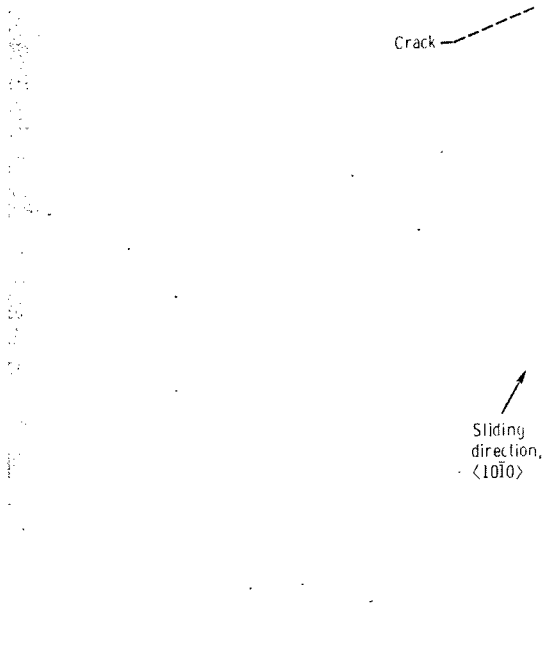

(a) Load, 30 grams.

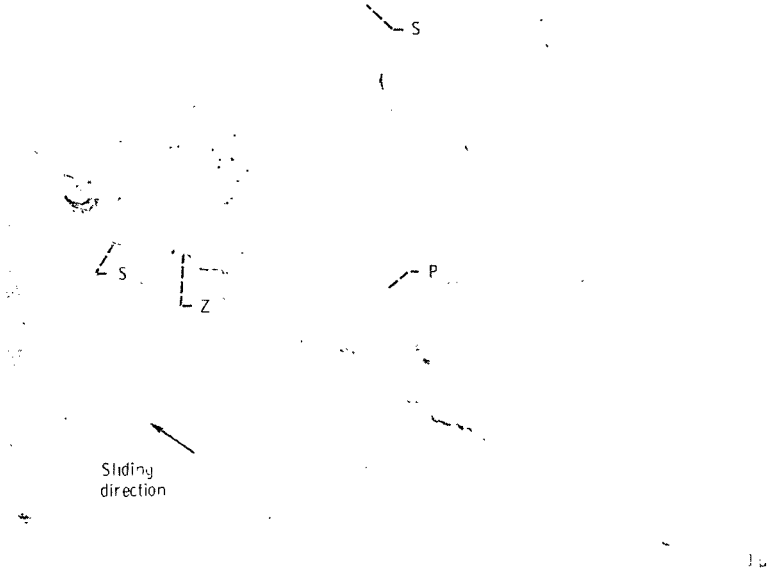

(b) Load, 40 grams.

Figure 4. - Replication electron micrographs of wear track on polished (0001) silicon carbide surface. Single pass of 0.02-mm-radius spherical diamond rider in argon at atmospheric pressure; sliding direction, $\langle 10\bar{1}0 \rangle$; sliding velocity, 3 mm/min; temperature, 25° C.

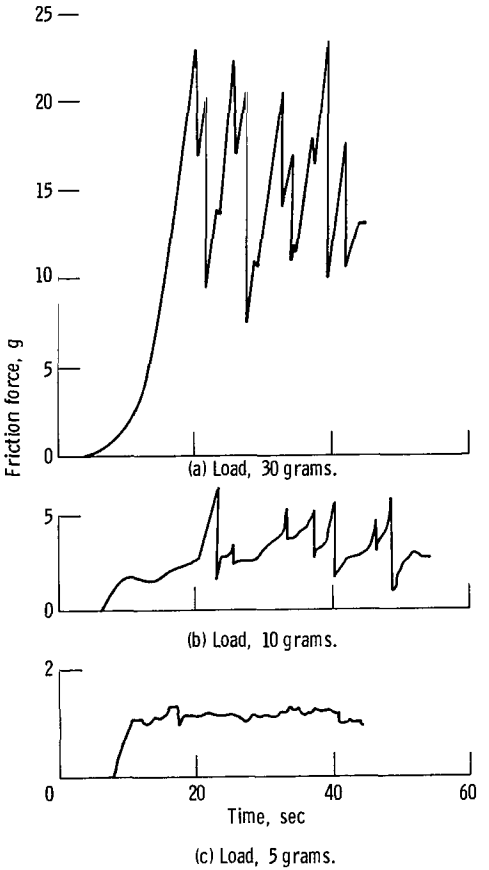

Figure 5. - Friction traces for conical diamond rider sliding on silicon carbide (0001) single-crystal surfaces in argon at atmospheric pressure. Sliding direction, $\langle 10\bar{1}0 \rangle$; sliding velocity, 3 mm/min; temperature, 25^0 C.

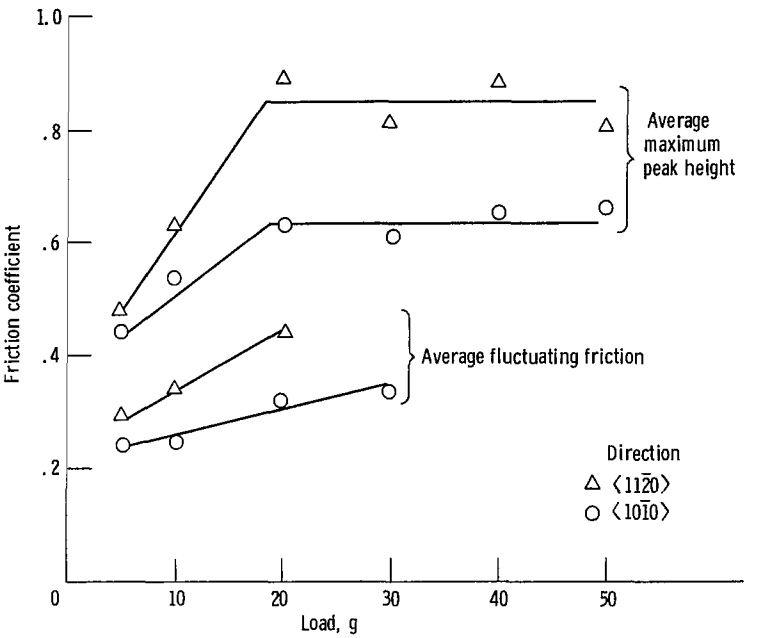

Figure 6. - Friction coefficient as function of load for conical diamond rider sliding on silicon carbide (0001) single-crystal surfaces in argon at atmospheric pressure. Sliding velocity, 3 mm/min; temperature, 25^0 C.

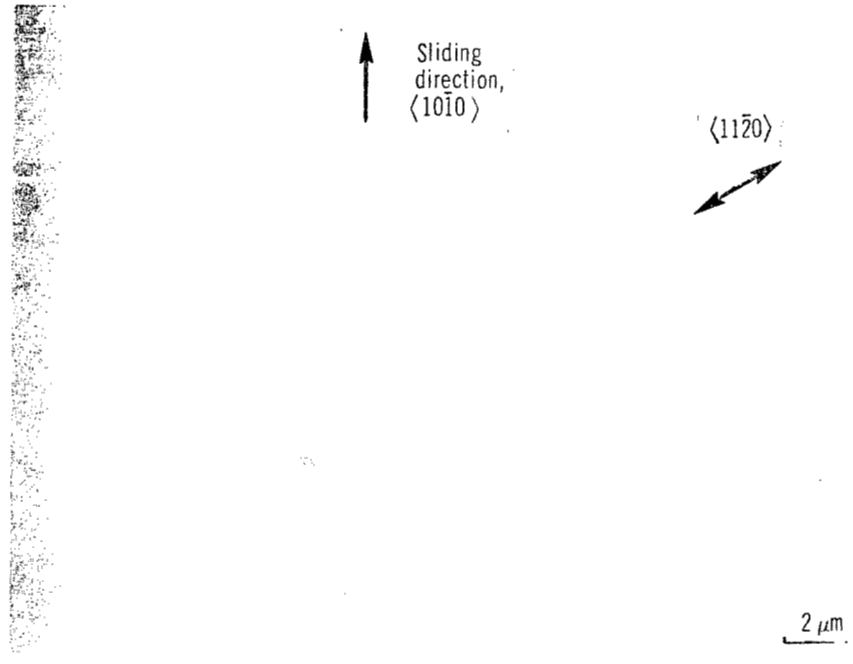

(a) Scanning electron micrograph.

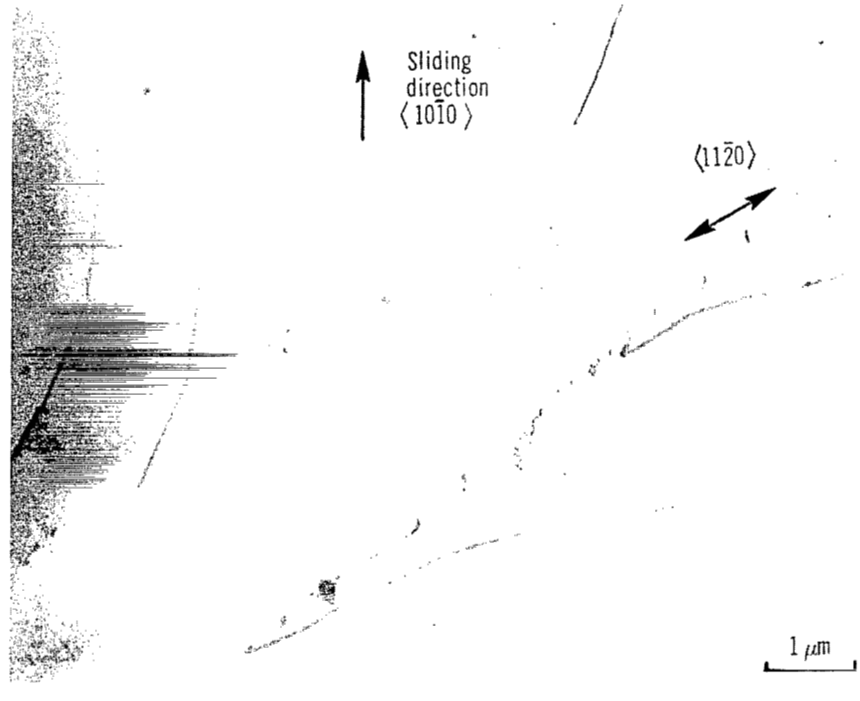

(b) Replication electron micrograph.

Figure 7. - Wear track on polished (0001) silicon carbide surface. Single pass of conical diamond rider in argon at atmospheric pressure; sliding direction, ⟨10$\bar{1}$0⟩; sliding velocity, 3 mm/min; load, 30 grams; temperature, 25° C.

(a) Wear track.

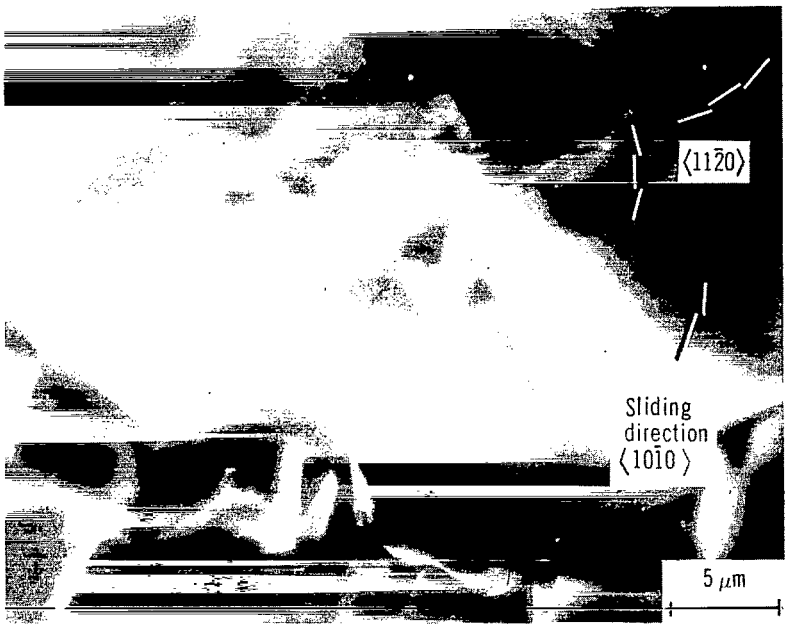

(b) Wear track at higher magnification.

Figure 8. - Scanning electron micrographs of wear track on polished (0001) silicon carbide surface. Single pass of conical diamond rider in argon at atmospheric pressure; sliding direction, ⟨10$\bar{1}$0⟩; sliding velocity, 3 mm/min; load, 50 grams; temperature, 25° C.

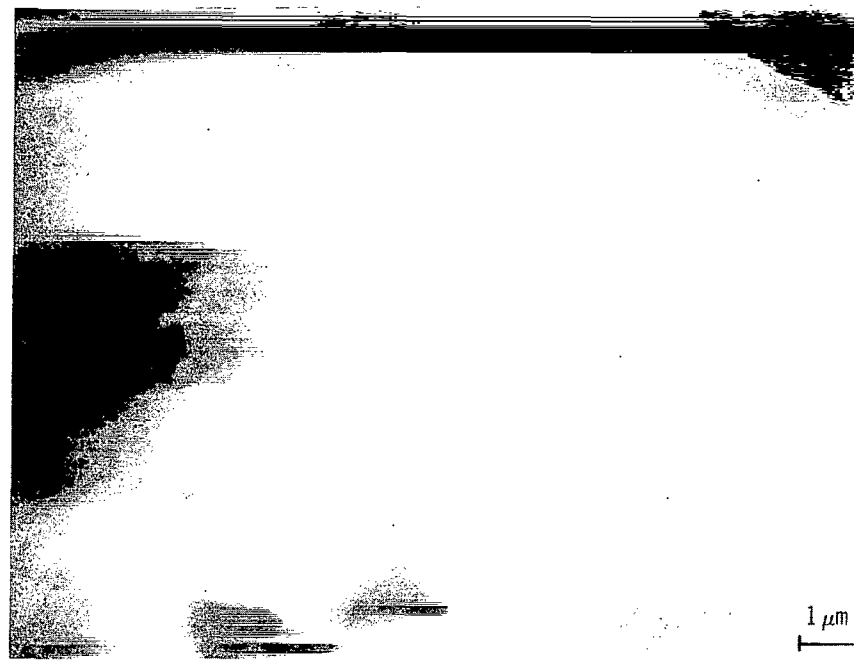

(c) Cleavage surface.

Figure 8. - Concluded.

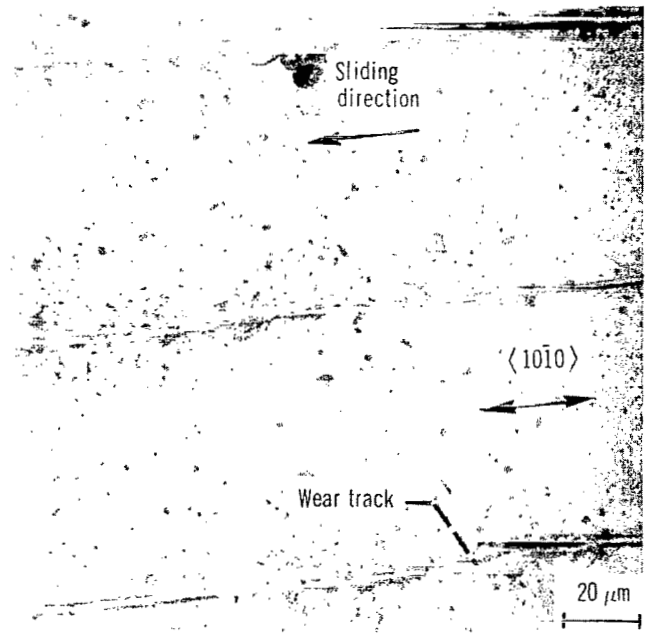

(a) ⟨10$\bar{1}$0⟩ direction.

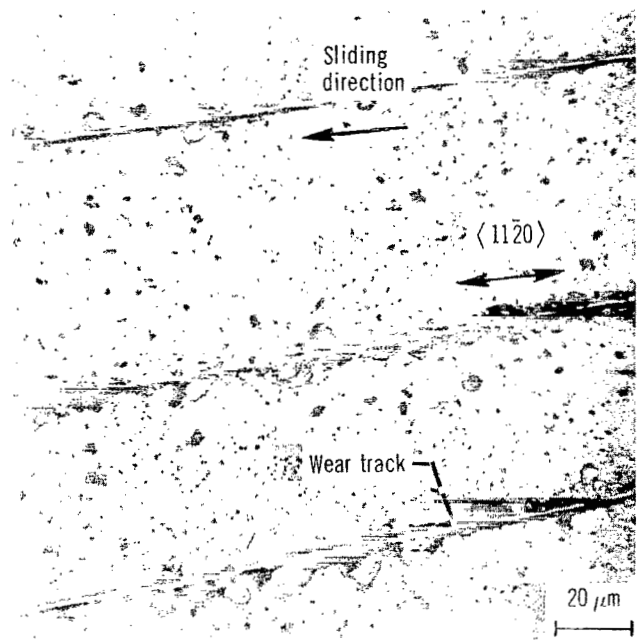

(b) ⟨11$\bar{2}$0⟩ direction.

Figure 9. - Optical micrographs of wear debris of silicon carbide. Single pass of conical diamond rider in argon at atmospheric pressure; sliding directions, ⟨10$\bar{1}$0⟩ and ⟨11$\bar{2}$0⟩; sliding velocity, 3 mm/min; load, 30 grams; temperature, 25° C.

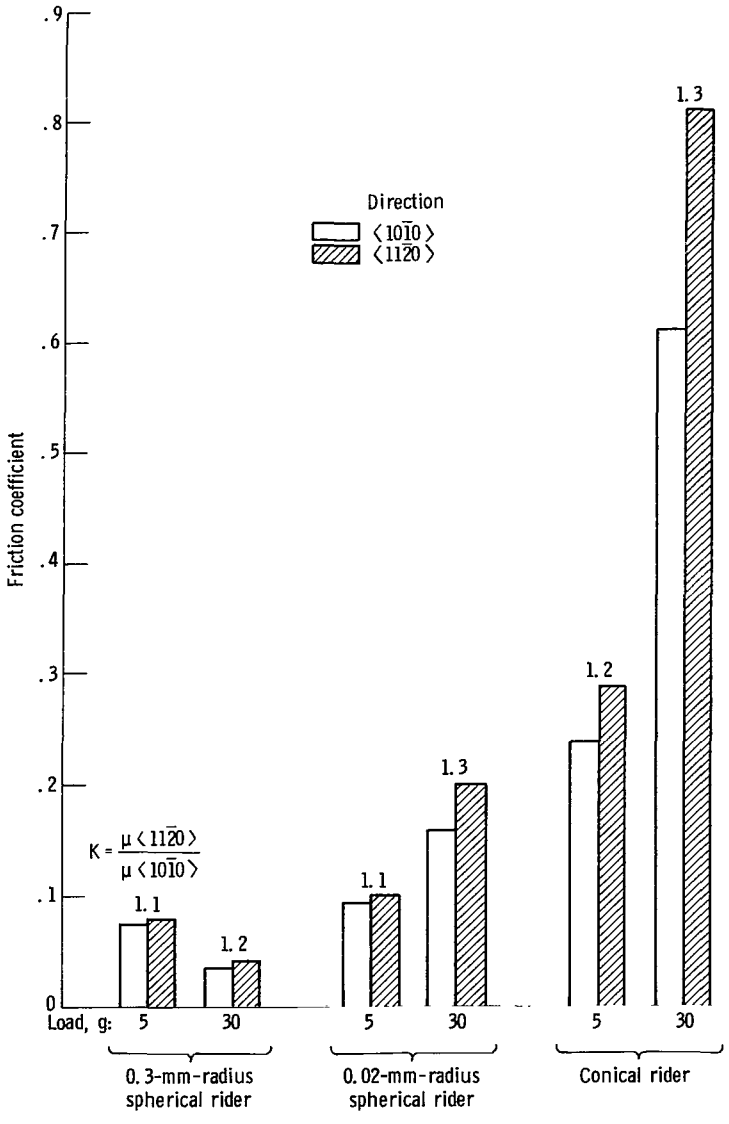

Figure 10. - Friction anisotropy for spherical and conical diamond riders sliding on silicon carbide (0001) single-crystal surface in argon at atmospheric pressure. Sliding velocity, 3 mm/min; temperature, 25° C.

Figure 11. - Scanning electron micrographs of wear tracks on polished (0001) silicon carbide surface (etched with molten salt ($1NaF + 2KCO_3$) at 700° to 800° C). Single pass of conical diamond rider in argon at atmospheric pressure; sliding direction, ⟨10$\bar{1}$0⟩; sliding velocity, 3 mm/min; load, 50 grams; temperature, 25° C.

Figure 11. - Concluded.

1. Report No.	2. Government Accession No.	3. Recipient's Catalog No.
NASA TP-1053		

4. Title and Subtitle

FRICTION AND DEFORMATION BEHAVIOR OF SINGLE-CRYSTAL SILICON CARBIDE

5. Report Date: October 1977

6. Performing Organization Code

7. Author(s)

Kazuhisa Miyoshi and Donald H. Buckley

8. Performing Organization Report No.: E-9121

9. Performing Organization Name and Address

National Aeronautics and Space Administration
Lewis Research Center
Cleveland, Ohio 44135

10. Work Unit No.: 506-16

11. Contract or Grant No.

12. Sponsoring Agency Name and Address

National Aeronautics and Space Administration
Washington, D. C. 20546

13. Type of Report and Period Covered: Technical Paper

14. Sponsoring Agency Code

15. Supplementary Notes

16. Abstract

Friction and deformation studies were conducted with single-crystal silicon carbide in sliding contact with diamond. When the radius of curvature of the spherical diamond rider was large (0.3 mm), deformation of silicon carbide was primarily elastic. Under these conditions the friction coefficient was low and did not show a dependence on the silicon carbide orientation. Further, there was no detectable cracking of the silicon carbide surfaces. When smaller radii of curvature of the spherical diamond riders (0.15 and 0.02 mm) or a conical diamond rider was used, plastic grooving occurred and the silicon carbide exhibited anisotropic friction and deformation behavior. Under these conditions the friction coefficient depended on load. Anisotropic friction and deformation of the basal plane of silicon carbide was controlled by the slip system $\{10\bar{1}0\}\langle 11\bar{2}0\rangle$ and cleavage of $\{10\bar{1}0\}$.

17. Key Words (Suggested by Author(s))	18. Distribution Statement
Single-crystal silicon carbide; Friction; Elastic and plastic deformation; Fracture; Anisotropic friction and deformation	Unclassified - unlimited STAR Category 27

19. Security Classif. (of this report)	20. Security Classif. (of this page)	21. No. of Pages	22. Price*
Unclassified	Unclassified	21	A02

* For sale by the National Technical Information Service, Springfield, Virginia 22161

NASA-Langley, 1977

1 1 1U,C, 092377 S00903DS
DEPT OF THE AIR FORCE
AF WEAPONS LABORATORY
ATTN: TECHNICAL LIBRARY (SUL)
KIRTLAND AFB NM 87117